eLIFE elifesciences.org

RESEARCH ARTICLE

Figures and figure supplements

ErbB4 deletion in noradrenergic neurons in the locus coeruleus induces mania-like behavior via elevated catecholamines

Shu-Xia Cao *et al*

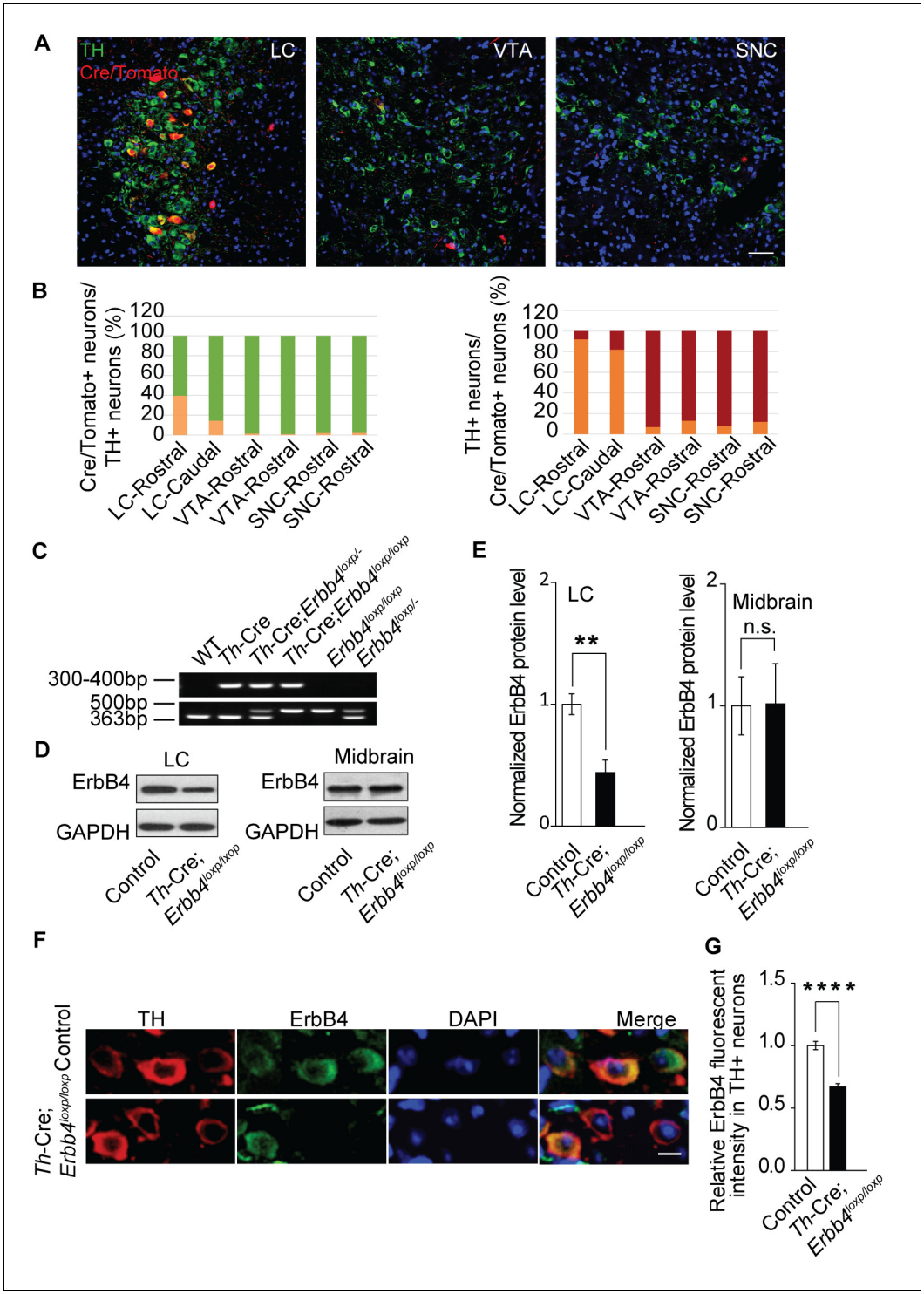

Figure 1. ErbB4 is primarily deleted in NE neurons of the LC in *Th-Cre;Erbb4*$^{loxp/loxp}$ mice. (**A**) Representative micrographs of Cre/Tomato distribution (red) in the locus coeruleus (LC), ventral tegmental area (VTA), and substantia nigra pars compacta (SNC). Slices were obtained from Ai9;*Th-Cre* mice and stained with antibody to TH (green), a marker of NE and dopaminergic neurons. Scale bar, 50 µm. (**B**) Colocalization of TH and Cre/Tomato. Three mice were studied, with three slices chosen for each mouse. (**C**) Genotyping of *Th-Cre;Erbb4*$^{loxp/loxp}$ mice. The *Erbb4* primers generated a 363-base pair (bp) product for the wild-type allele or a 500 bp product for the loxP-flanked allele. The *Th-Cre* primers generated a band between 300 and 400 bp. (**D**), (**E**) Quantification of the fold change in ErbB4 protein expression relative to control mice. Unpaired two-tailed Student's t-test. Data are

Figure 1 continued on next page

Figure 1 continued

expressed as means ± s.e.m. **p<0.01. (**F**) Specific deletion of ErbB4 in NE neurons of the LC. Sections from *Th-Cre* mice and *Th-Cre;Erbb4*$^{loxp/loxp}$ mice were stained with ErbB4-specific antibody and TH-specific antibody. Sections were also stained with DAPI to indicate nuclei. Scale bar, 10 μm. (**G**) Quantification of ErbB4 fluorescent intensity in TH-positive (TH+) cells. n = 13 slices (control), random 16 – 30 TH+ cells were quantified from each slice. n = 11 slices (*Th-Cre;Erbb4*$^{loxp/loxp}$), random 19 – 30 TH+ cells were quantified from each slice.

DOI: https://doi.org/10.7554/eLife.39907.003

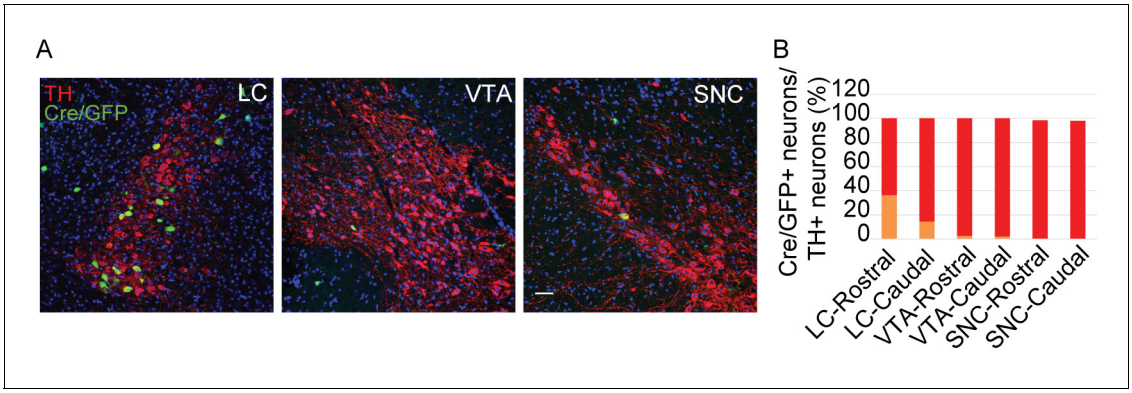

Figure 1—figure supplement 1. Cre/GFP was primarily expressed in NE neurons of the LC in Ai3;*Th-Cre* mice. (**A**) Representative micrographs of Cre/GFP distribution (green) in Ai3;*Th-Cre* mice. Locus coeruleus (LC), ventral tegmental area (VTA), and substantia nigra pars compacta (SNC) slices were obtained from Ai3;*Th-Cre* mice and stained with antibody to TH (red), a marker of NE and dopaminergic neurons. Scale bar, 50 μm. (**B**) Cartogram of Cre expression in TH-positive neurons in the LC, VTA, and SNC. Three mice were studied, with three slices for each mouse.

DOI: https://doi.org/10.7554/eLife.39907.004

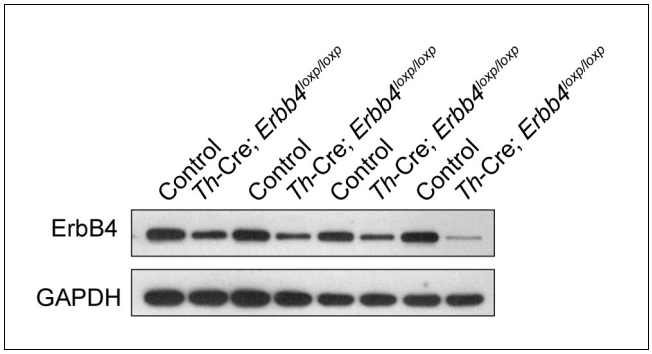

Figure 1—figure supplement 2. ErbB4 was primarily deleted in the LC of *Th-Cre;Erbb4*$^{loxp/loxp}$ mice. Shown are representative Western blots of the ErbB4 protein (180 kDa) in *Th-Cre;Erbb4*$^{loxp/loxp}$ mice. *Erbb4*$^{loxp/loxp}$ mice and *Th-Cre* mice were used as controls. n = 4 (control); n = 4 (*Th-Cre;Erbb4*$^{loxp/loxp}$).

DOI: https://doi.org/10.7554/eLife.39907.005

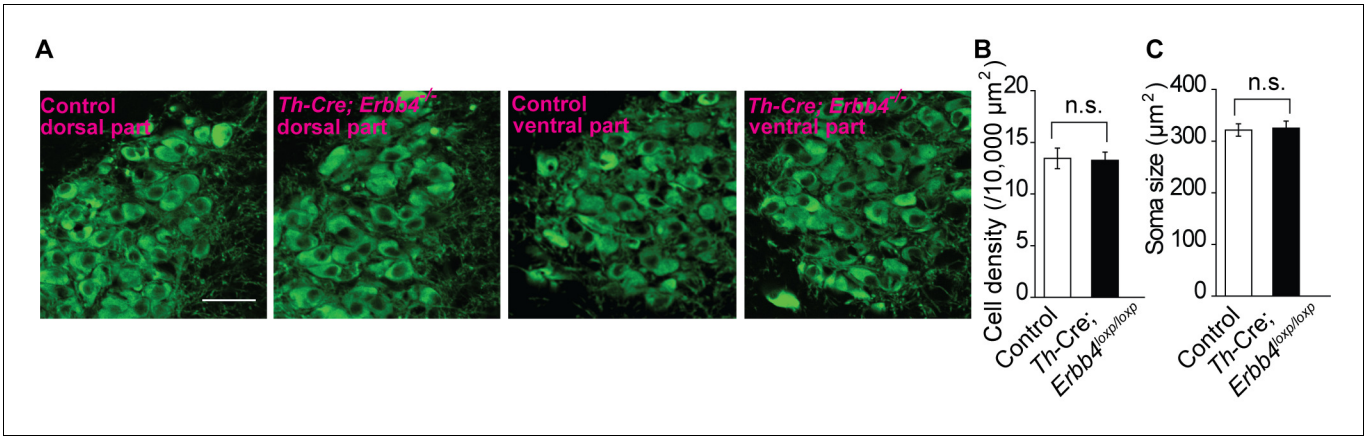

Figure 1—figure supplement 3. No obvious differences were detected in cell density or soma size of LC neurons between control and *Th-Cre; Erbb4*$^{loxp/loxp}$ mice. (**A**) Representative micrographs of LC neurons in the dorsal and ventral parts of the LC in control and *Th-Cre;Erbb4*$^{loxp/loxp}$ mice. Coronal LC slices were obtained from control and *Th-Cre;Erbb4*$^{loxp/loxp}$ mice and were stained with antibody to TH (green), a marker of NE and dopaminergic neurons. Scale bar, 50 μm. (**B**), (**C**) Cell density and soma size of LC neurons did not differ significantly between control and *Th-Cre; Erbb4*$^{loxp/loxp}$ mice. Unpaired two-tailed Student's t-test. Data are expressed as means ± s.e.m. n.s., not significant.

DOI: https://doi.org/10.7554/eLife.39907.006

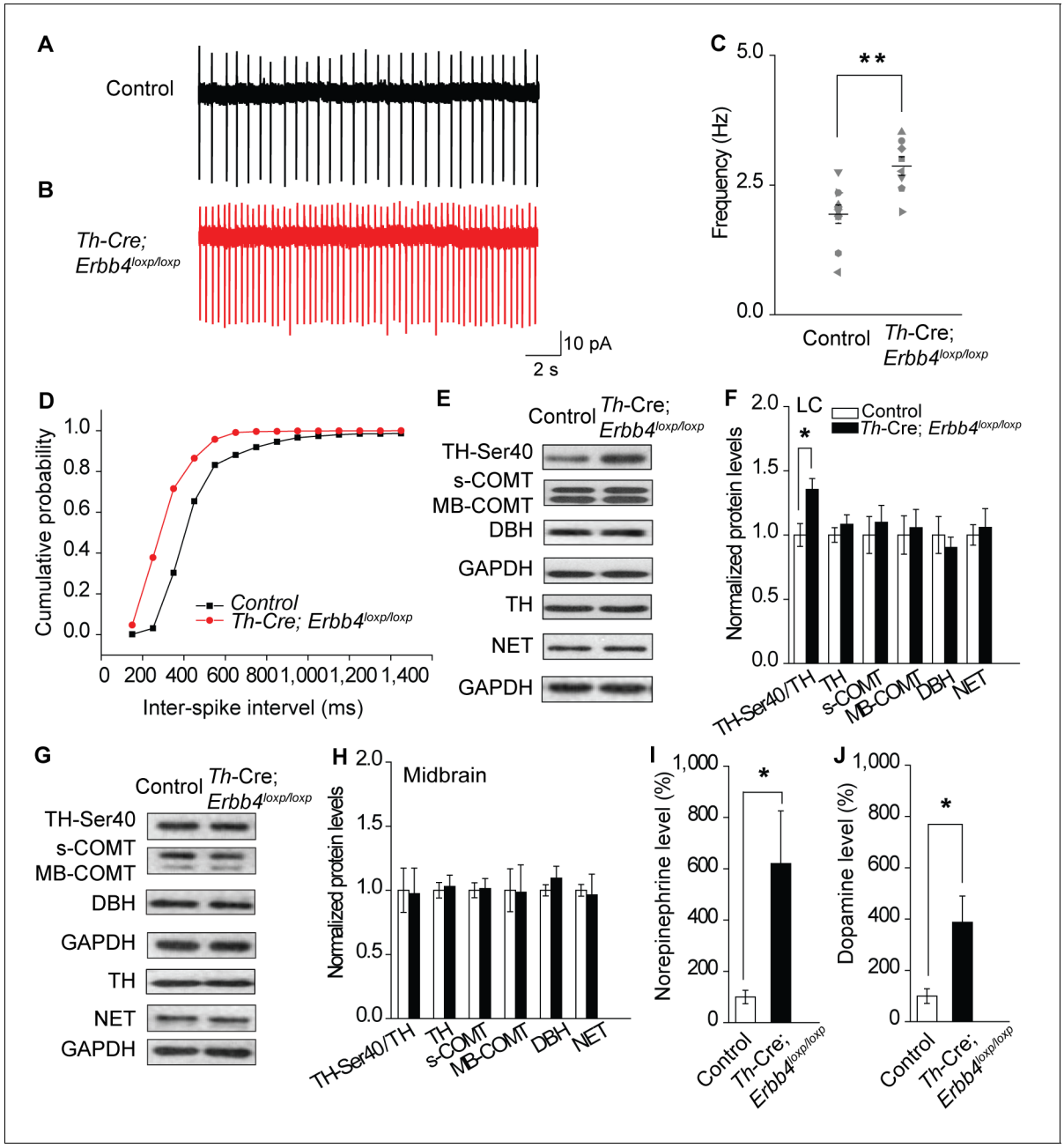

Figure 2. Increased spontaneous firing of LC-NE neurons, extracellular norepinephrine, and intracellular TH phosphorylation in *Th-Cre;Erbb4*$^{loxp/loxp}$ mice. (**A**), (**B**) Representative firing of LC-NE neurons from control (black) and *Th-Cre;Erbb4*$^{loxp/loxp}$ mice (red). (**C**) Spontaneous firing frequency of LC-NE neurons was increased in *Th-Cre;Erbb4*$^{loxp/loxp}$ mice. n = 10 from three mice (control); n = 8 from three mice (*Th-Cre;Erbb4*$^{loxp/loxp}$). (**D**) Interspike intervals were calculated over 2 min of firing from each neuron. Interspike intervals were decreased in *Th-Cre;Erbb4*$^{loxp/loxp}$ mice compared with control mice. n = 10 from three mice (control); n = 8 from three mice (*Th-Cre;Erbb4*$^{loxp/loxp}$). Two-sample Kolmogorov-Smirnov test and data in (**D**) are presented in a cumulative frequency plot. ****p<0.0001. (**E**), (**F**) Protein levels of TH-Ser40 were increased in the LC of *Th-Cre;Erbb4*$^{loxp/loxp}$ mice. NET, norepinephrine reuptake transporter; DBH, dopamine beta-hydroxylase; S-COMT, soluble catechol-o-methyltransferase; MB-COMT, membrane-binding form of COMT. (**G**), (**H**) No significant change was detected in the dopaminergic neurons clustered in the midbrain (VTA and SNC). (**I**), (**J**) In vivo microdialysis and HPLC data suggested that norepinephrine and dopamine levels were significantly increased in *Th-Cre;Erbb4*$^{loxp/loxp}$ mice. Standard curves are presented in ***Figure 2—figure supplement 2***. n = 6 mice (control); n = 6 mice (*Th-Cre;Erbb4*$^{loxp/loxp}$). Unpaired two-tailed Student's t-test. Data are expressed as means ± s.e.m. *p<0.05.

DOI: https://doi.org/10.7554/eLife.39907.008

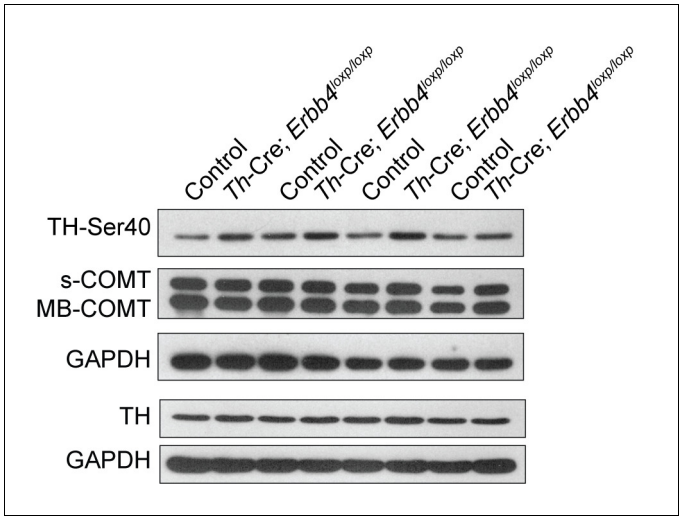

Figure 2—figure supplement 1. Representative Western blots of TH and COMT in the LC of control and *Th-Cre; Erbb4*$^{loxp/loxp}$ mice. Ser40 phosphorylation of tyrosine hydroxylase (TH-Ser40), tyrosine hydroxylase (TH), soluble catechol-o-methyltransferase (s-COMT), membrane-bound form of COMT (MB-COMT). n = 4 (control); n = 4 (*Th-Cre;Erbb4*$^{loxp/loxp}$).

DOI: https://doi.org/10.7554/eLife.39907.009

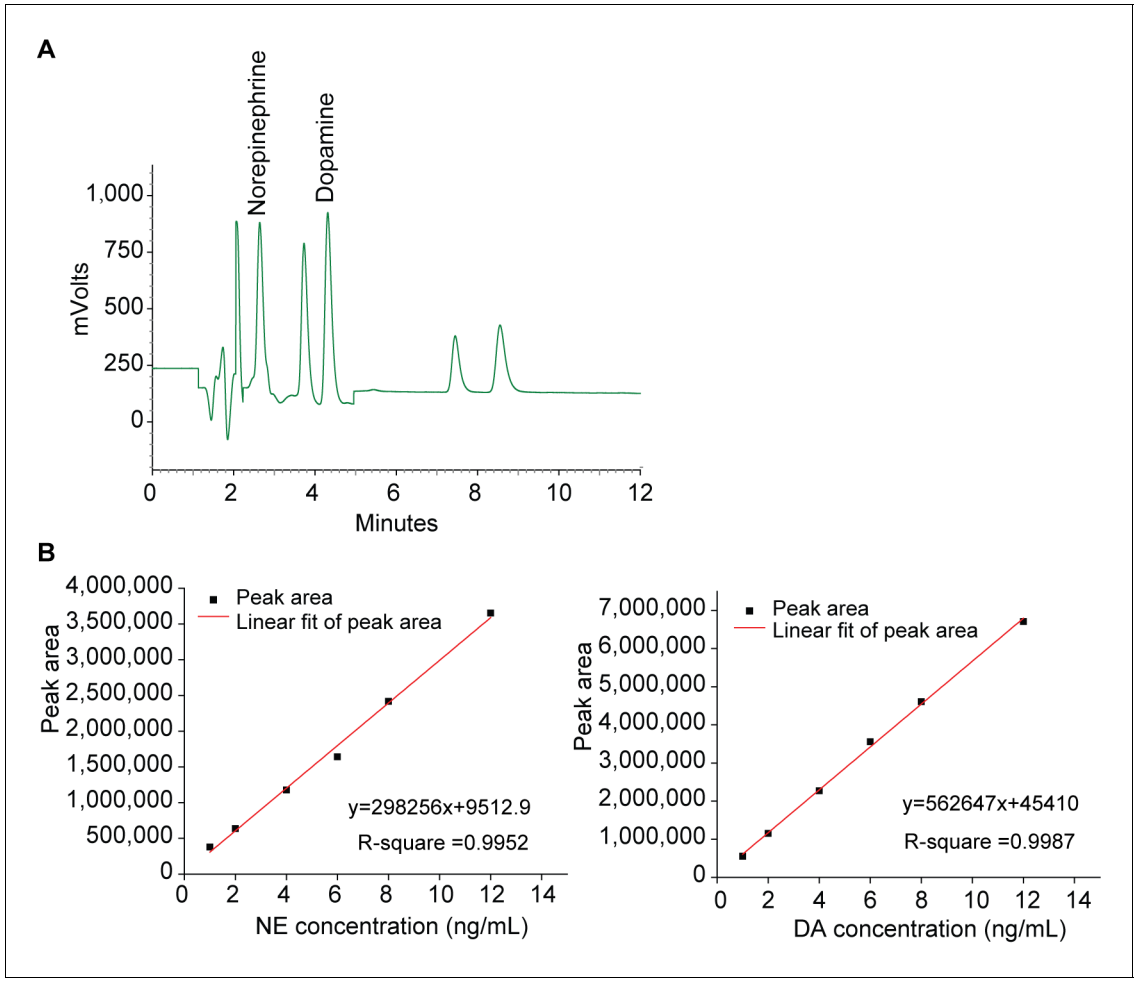

Figure 2—figure supplement 2. HPLC analysis of norepinephrine and dopamine. (**A**) Representative graphs of main peaks in HPLC chromatograms. Norepinephrine; Dopamine. X-axis, retention time. (**B**) Standard curves of norepinephrine (NE) and dopamine (DA).

DOI: https://doi.org/10.7554/eLife.39907.010

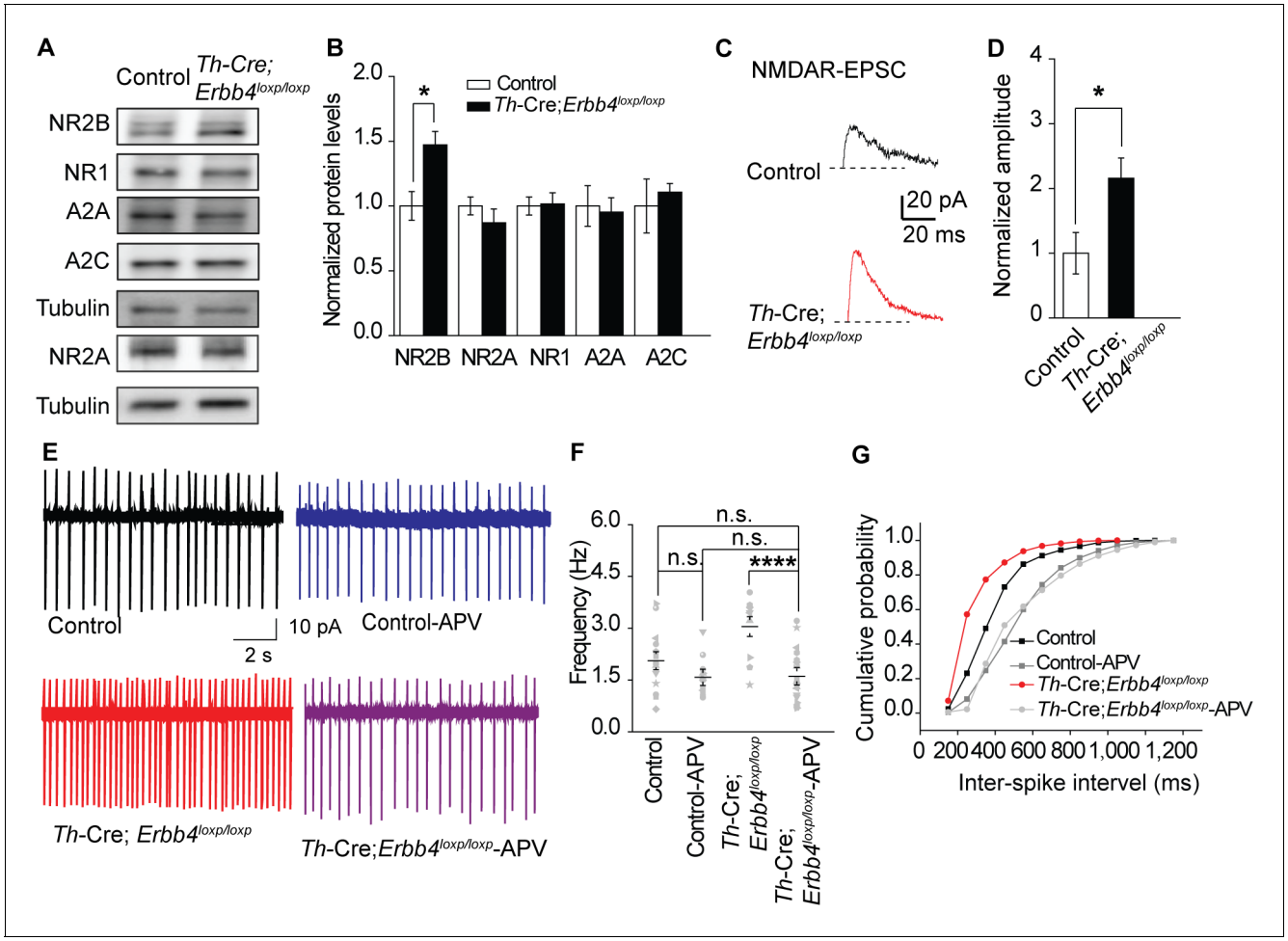

Figure 3. NMDA receptor mediates hyperexcitability of LC-NE neurons in *Th-Cre;Erbb4*$^{loxp/loxp}$ mice. (**A**), (**B**) Protein levels of NMDA receptor subunit NR2B were increased in the LC of *Th-Cre;Erbb4*$^{loxp/loxp}$ mice. Unpaired two-tailed Student's t-test. Data are expressed as means ± s.e.m. *p<0.05. (**C**) Representative NMDAR-EPSC current traces from LC-NE neurons in *Ai9;Th-Cre* (control) and *Ai9; Th-Cre;Erbb4*$^{loxp/loxp}$ mice. (**D**) Amplitude of NMDAR current recorded in LC-NE neurons is significantly increased in ErbB4-deficient mice compared with control mice. n = 7 from three mice (control); n = 8 from three mice (*Th-Cre;Erbb4*$^{loxp/loxp}$). (**E**) Representative firing of LC-NE neurons from control and *Th-Cre;Erbb4*$^{loxp/loxp}$ mice untreated or treated with APV (50 μM), an NMDA receptor antagonist. (**F**) Spontaneous firing frequency of LC-NE neurons was rescued by APV (50 μM) in *Th-Cre;Erbb4*$^{loxp/loxp}$ mice. n = 13 from three mice (*Th-Cre;Erbb4*$^{loxp/loxp}$); n = 20 from three mice (*Th-Cre;Erbb4*$^{loxp/loxp}$ + APV). Two-way ANOVA. Data are expressed as means ± s.e.m. *p<0.05. (**G**) Inter-spike intervals were significantly rescued by APV (50 μM) in *Th-Cre;Erbb4*$^{loxp/loxp}$ mice. n = 13 from three mice (*Th-Cre;Erbb4*$^{loxp/loxp}$); n = 20 from three mice (*Th-Cre;Erbb4*$^{loxp/loxp}$ + APV). Two-sample Kolmogorov-Smirnov test and data in (**G**) are presented in a cumulative frequency plot. ***p<0.001.

DOI: https://doi.org/10.7554/eLife.39907.012

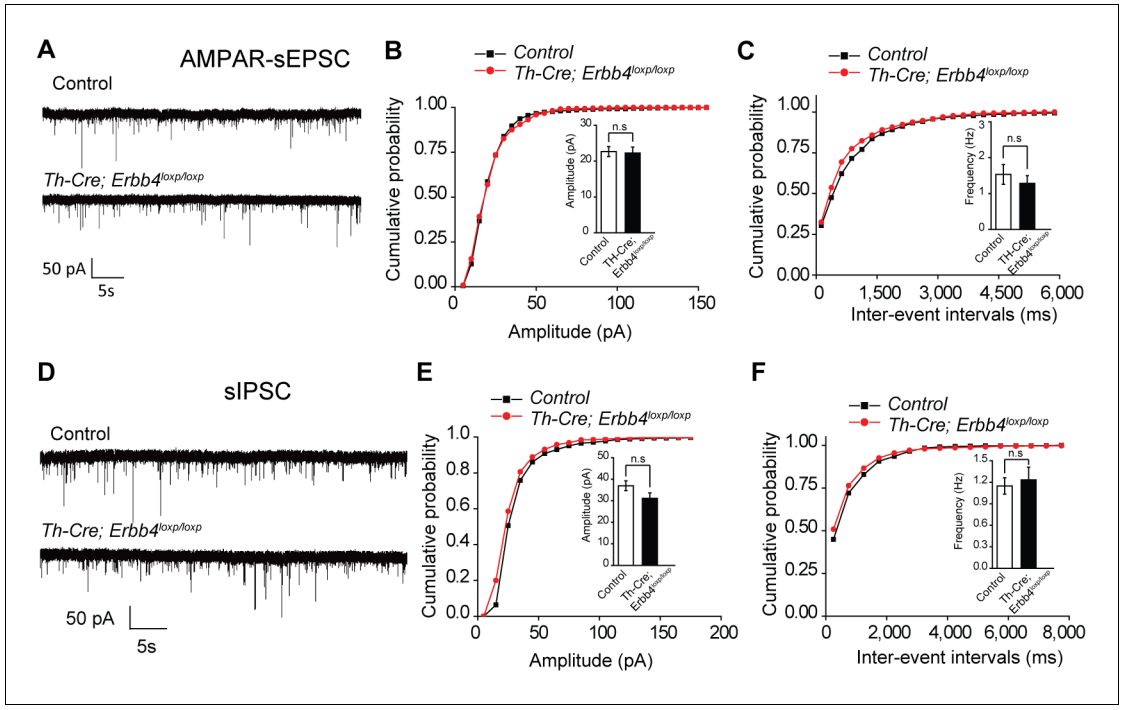

Figure 3—figure supplement 1. Spontaneous excitation and inhibition balance measured by sEPSC and sIPSC is not changed in LC-NE neurons of *Th-Cre;Erbb4$^{loxp/lox}$* mice. (**A**) Representative sEPSC traces of LC-NE neurons in control (*Erbb4$^{loxp/loxp}$*) mice and *Th-Cre;Erbb4$^{loxp/loxp}$* mice. (**B**), (**C**) No significant change in the amplitude (**B**) and inter-event intervals (**C**) of LC-NE neuron sEPSC in control mice and *Th-Cre;Erbb4$^{loxp/lox}$* mice. n = 8 from three mice (control); n = 10 from three mice (*Th-Cre;Erbb4$^{loxp/loxp}$*). (**D**) Representative sIPSC traces of LC-NE neurons in control mice and *Th-Cre; Erbb4$^{loxp/lox}$* mice. (**E**), (**F**) No significant change in the amplitude (**E**) and inter-event intervals (**F**) of LC-NE neuron sEPSC in control mice and *Th-Cre; Erbb4$^{loxp/lox}$* mice. n = 13 from three mice (control); n = 11 from three mice (*Th-Cre;Erbb4$^{loxp/lox}$*). Unpaired two-tailed Student's t-test and Two-sample Kolmogorov-Smirnov test. Data are expressed as means ± s.e.m. n.s., not significant.

DOI: https://doi.org/10.7554/eLife.39907.013

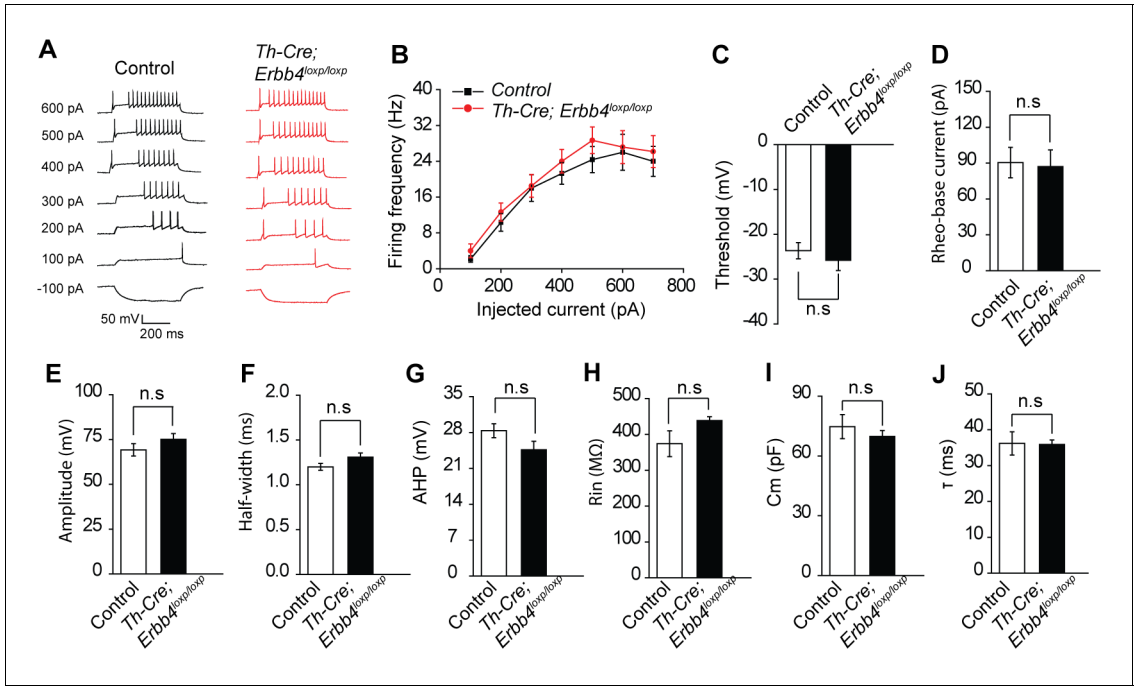

Figure 3—figure supplement 2. Intrinsic properties of LC-NE neurons are unchanged in *Th-Cre; ErbB4$^{loxp/loxp}$* mice. (**A**) Representative voltage response of LC-NE neurons to injected currents ranging from −100 pA to 600 pA at 100 pA step size. (**B**) Summary histogram of LC-NE neuron voltage response of control (*Erbb4$^{loxp/loxp}$*) mice and *Th-Cre; ErbB4$^{loxp/loxp}$* mice. (**C–G**) Positive membrane properties, including threshold (**C**) rheo-base current (**D**) amplitude (**E**) half-width (**F**) and afterhyperpolarization (AHP) (**G**) show no significant difference in the mutants compared with control mice. (**H–J**) Normal input resistance (**H**) membrane capacitance (**I**) and time constant (**J**) in LC-NE neurons in *Th-Cre; ErbB4$^{loxp/loxp}$* mice. n = 6 from three mice (control); n = 8 from three mice (*Th-Cre; ErbB4$^{loxp/loxp}$*). Unpaired two-tailed Student's t-test. Data are expressed as means ± s.e.m. n.s., not significant.

DOI: https://doi.org/10.7554/eLife.39907.014

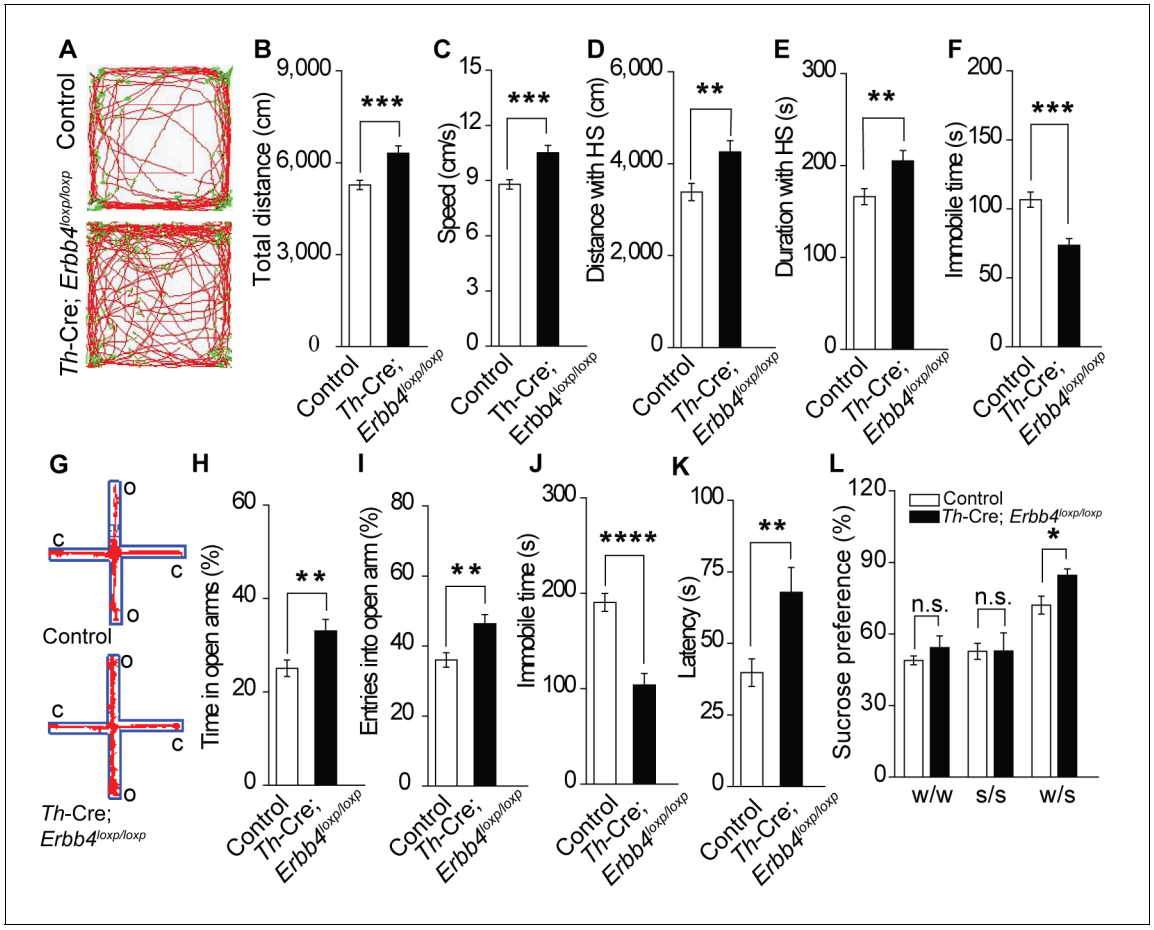

Figure 4. *Th-Cre;Erbb4*$^{loxp/loxp}$ mice show mania-like behaviors. (**A**) Representative trajectories of control (*Erbb4*$^{loxp/loxp}$) and *Th-Cre;Erbb4*$^{loxp/loxp}$ mice. We defined high speed (red line) as >10 cm/s, immobility as <2 cm/s, and low speed (green line) as 2 – 10 cm/s. (**B**), (**C**) Locomotor activity (**B**) and speed (**C**) of control and *Th-Cre;Erbb4*$^{loxp/loxp}$ mice in open field tests. n = 24 (control); n = 22 (*Th-Cre;Erbb4*$^{loxp/loxp}$). (**D**), (**E**) Distance (**D**) and duration (**E**) traveled at high speed (HS). n = 17 (control); n = 13 (*Th-Cre;Erbb4*$^{loxp/loxp}$). (**F**) Immobility time during open field tests decreased in *Th-Cre;Erbb4*$^{loxp/loxp}$ mice. (**G**) Examples of the performance of control and *Th-Cre;Erbb4*$^{loxp/loxp}$ mice in the EPM test. C, closed arm; O, open arm. (**H**), (**I**) Performance of control and *Th-Cre;Erbb4*$^{loxp/loxp}$ mice in the EPM test. n = 34 (control); n = 24 (*Th-Cre;Erbb4*$^{loxp/loxp}$). (**J**), (**K**) Immobility time (**J**) and latency to first surrender (**K**) in the forced swim test. n = 22 (control); n = 13 (*Th-Cre;Erbb4*$^{loxp/loxp}$). (**L**) Sucrose preference of control and *Th-Cre;Erbb4*$^{loxp/loxp}$ mice. Water (w). Sucrose (s). n = 19 (control); n = 14 (*Th-Cre;Erbb4*$^{loxp/loxp}$). Unpaired two-tailed Student's t-test. Data are expressed as means ± s.e.m. *p<0.05, **p<0.01, ***p<0.001, ****p<0.0001. n.s., not significant.

DOI: https://doi.org/10.7554/eLife.39907.016

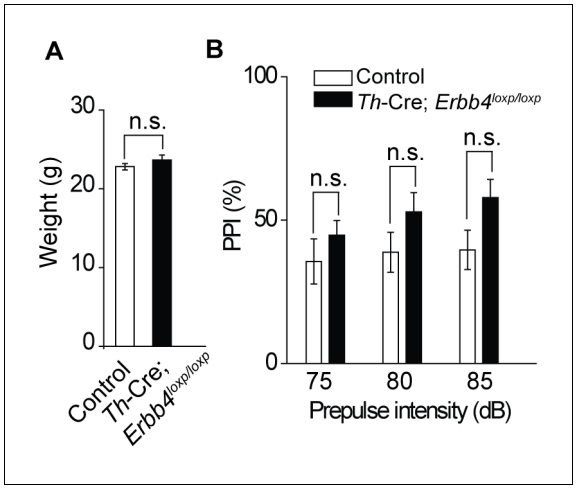

Figure 4—figure supplement 1. There was no significant difference in body weight between control and *Th-Cre;Erbb4*$^{loxp/loxp}$ mice and no deficit of *Th-Cre; Erbb4*$^{loxp/loxp}$ mice in the prepulse inhibition experiment. (**A**) No significant differences in body weight were detected between control and *Th-Cre; Erbb4*$^{loxp/loxp}$ mice. n = 7 (control); n = 8 (*Th-Cre; Erbb4*$^{loxp/loxp}$). (**B**) No prepulse inhibition deficit was observed in *Th-Cre;Erbb4*$^{loxp/loxp}$ mice. n = 10 (control); n = 10 (*Th-Cre; Erbb4*$^{loxp/loxp}$). Unpaired two-tailed Student's t-test. Data are expressed as means ± s.e.m. *p<0.05. n.s., not significant.

DOI: https://doi.org/10.7554/eLife.39907.017

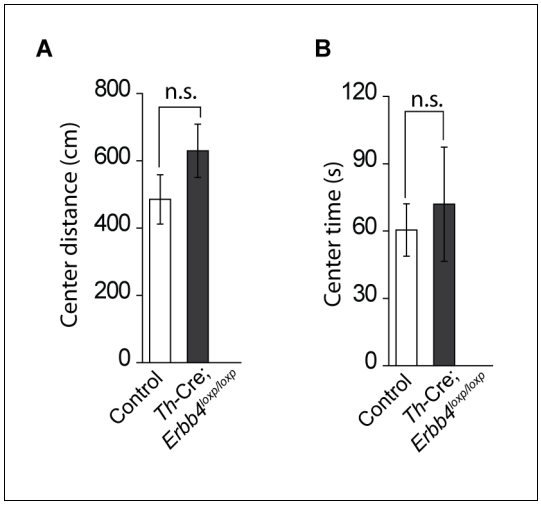

Figure 4—figure supplement 2. No significant change in the distance travelled in center and time spent in center area between control (*Erbb4*$^{loxp/loxp}$) mice and *Th-Cre; Erbb4*$^{loxp/loxp}$ mice in open field test. (**A**) Distance travelled in center area of control mice and *Th-Cre; Erbb4*$^{loxp/loxp}$ mice in open field test. n = 8 (control); n = 8 (*Th-Cre; Erbb4*$^{loxp/loxp}$). (**B**) Time spend in center area in open field test. n = 11 (control); n = 11 (*Th-Cre; Erbb4*$^{loxp/loxp}$). Unpaired two-tailed Student's t-test. Data are expressed as means ± s.e.m. n.s., not significant.

DOI: https://doi.org/10.7554/eLife.39907.018

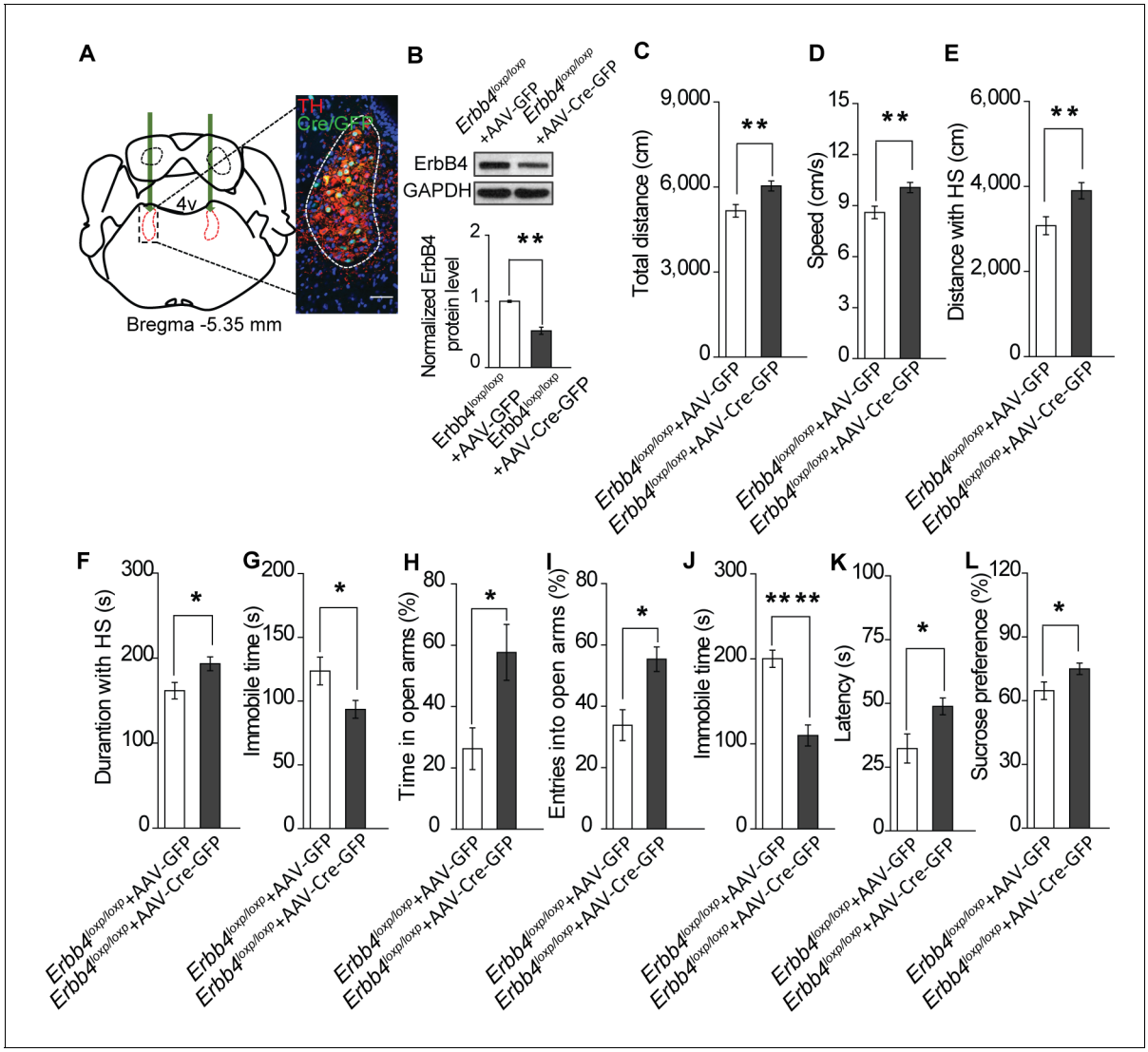

Figure 5. Specific ablation of ErbB4 in the LC is sufficient to cause mania-like behaviors. (**A**) Illustration of bilateral viral injection of AAV-Cre-GFP in the mouse LC. LC sections were examined for Cre/GFP (green) 5 weeks after stereotaxic microinjection of AAV-Cre-GFP into the LC of *Erbb4*$^{loxp/loxp}$ mice; antibody staining for TH is shown in red. Scale bars, 50 μm. Cartogram is presented in ***Figure 5—figure supplement 1*** . (**B**) ErbB4 expression detected by immunoblotting was significantly decreased in LC protein lysates from *Erbb4*$^{loxp/loxp}$ mice after AAV-Cre-GFP injection. n = 4 (AAV-GFP); n = 4 (AAV-Cre-GFP). (**C**, **D**) Locomotor activity (**C**) and speed (**D**) of mice injected with AAV-GFP or AAV-Cre-GFP in the open field test. n = 14 (AAV-GFP); n = 12 (AAV-Cre-GFP). (**E–G**) Distance (**E**) and duration (**F**) traveled at HS and immobility time (**G**) of mice in the open field test after viral injection. n = 14 (AAV-GFP); n = 12 (AAV-Cre-GFP). (**H**, **I**) Percentage of time (**H**) and entries (**I**) into the open arms by mice injected with AAV-GFP or AAV-Cre-GFP in the EPM test. n = 10 (AAV-GFP); n = 18 (AAV-Cre-GFP). (**J**, **K**) Immobility time (**J**) and latency to first surrender (**K**) in the forced swim test with AAV-GFP or AAV-Cre-GFP injection. n = 11 (AAV-GFP); n = 18 (AAV-Cre-GFP). (**L**) Sucrose preference of mice injected with AAV-GFP or AAV-Cre-GFP. n = 10 (AAV-GFP); n = 13 (AAV-Cre-GFP). Unpaired two-tailed Student's t-test. Data are expressed as means ± s.e.m. *p<0.05, **p<0.01, ****p<0.0001.
DOI: https://doi.org/10.7554/eLife.39907.020

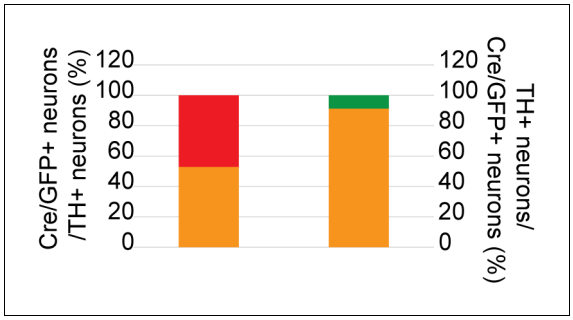

Figure 5—figure supplement 1. Cartogram of the colocalization of Cre/GFP-positive (Cre/GFP+) and NE neurons (TH+) in the LC 5 weeks after viral injection. Percentages of Cre/GFP+ neurons among NE neurons of the LC and of LC-NE neurons among Cre/GFP + neurons in *Erbb4*$^{loxp/loxp}$ mice after virus injection. Three mice were studied, with three slices for each mouse.

DOI: https://doi.org/10.7554/eLife.39907.021

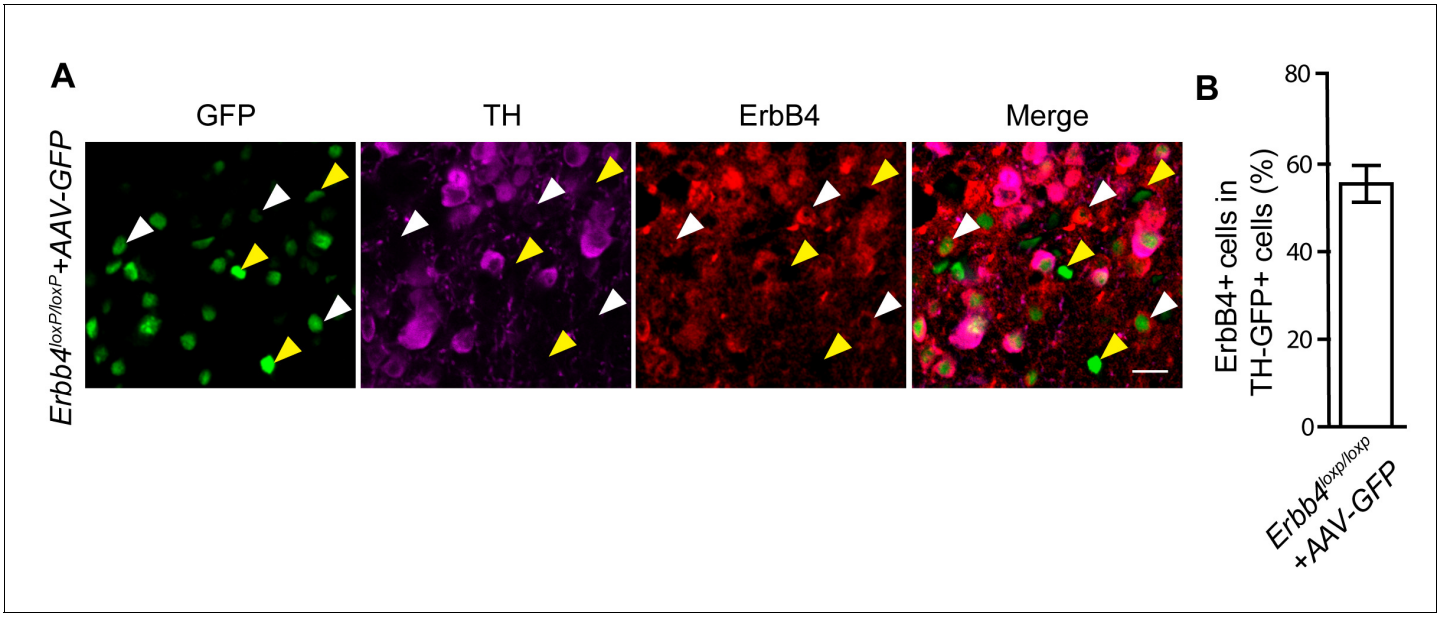

Figure 5—figure supplement 2. 55.5% of TH-GFP + neurons in AAV-injected *Erbb4*$^{loxp/loxp}$ mice are ErbB4+. (**A**) Representative image of GFP, TH, and ErbB4 colocalization in immunostained brain slice from *Erbb4*$^{loxp/loxp}$ mice injected with AAV-GFP in the LC. (**B**) Quantification of percentage of ErbB4 + cells in TH-GFP+ cells. White arrowhead: ErbB4 + TH-GFP+cells; Yellow arrowhead: ErbB4-TH-GFP + cells. n = 22 slices from three mice. Scale bar, 20 μm.

DOI: https://doi.org/10.7554/eLife.39907.022

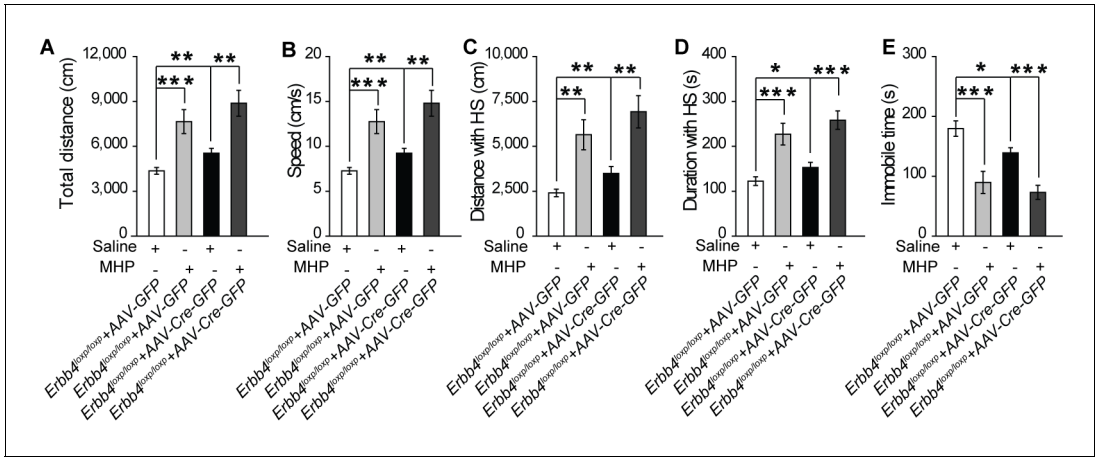

Figure 5—figure supplement 3. ErbB4-deficient mice are not an ADHD model. (**A**), (**B**) Total distance and speed in open field test are significantly increased in control (*Erbb4*$^{loxp/loxp}$) mice and *Th-Cre; Erbb4*$^{loxp/loxp}$ mice after MHP treatment. (**C–E**) Distance (**C**) and duration (**D**) traveled at HS and immobility time (**E**) after MHP treatment of MHP-treated control mice and *Th-Cre; Erbb4*$^{loxp/loxp}$ mice in open field test. n = 10 (control + Saline); n = 7 (*Th-Cre; Erbb4*$^{loxp/loxp}$ + Saline); n = 11 (control +MHP); n = 12 (*Th-Cre; Erbb4*$^{loxp/loxp}$ + MHP). Two-way ANOVA. Data are expressed as means ± s.e.m. *p<0.05, **p<0.01, ***p<0.001. n.s., not significant.

DOI: https://doi.org/10.7554/eLife.39907.023

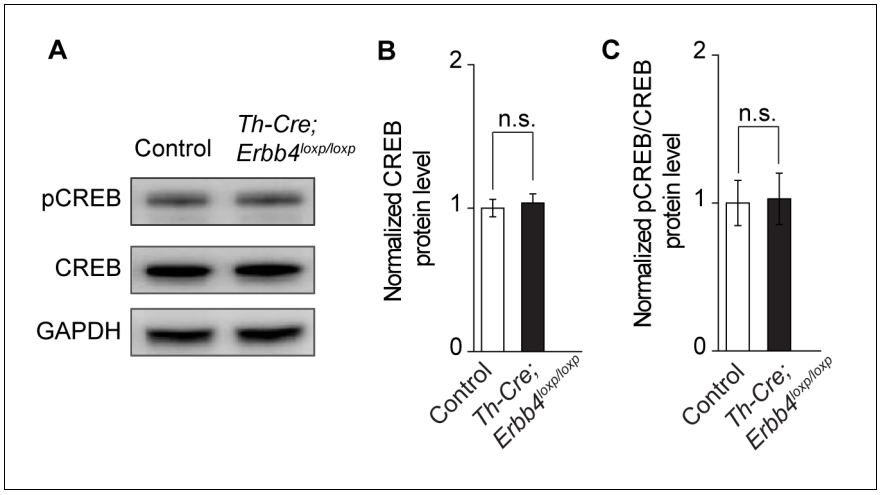

Figure 5—figure supplement 4. Normal CREB signaling activity in *Th-Cre;ErbB4$^{loxp/loxp}$* mice. (**A**) Representative blot of pCREB, CREB, and loading control GAPDH from LC protein lysates of *ErbB4$^{loxp/loxp}$* (Control) and *Th-Cre; ErbB4$^{loxp/loxp}$* mice. (**B**), (**C**) Quantification of relative ratio of total CREB to GAPDH (**B**) and pCREB to total CREB (pCREB/CREB) (**C**) in the LC of control and mutant mice. n = 6 (control); n = 6 (*Th-Cre; ErbB4$^{loxp/loxp}$*). Unpaired two-tailed Student's t-test. Data are expressed as means ± s.e.m. n.s., not significant.

DOI: https://doi.org/10.7554/eLife.39907.024

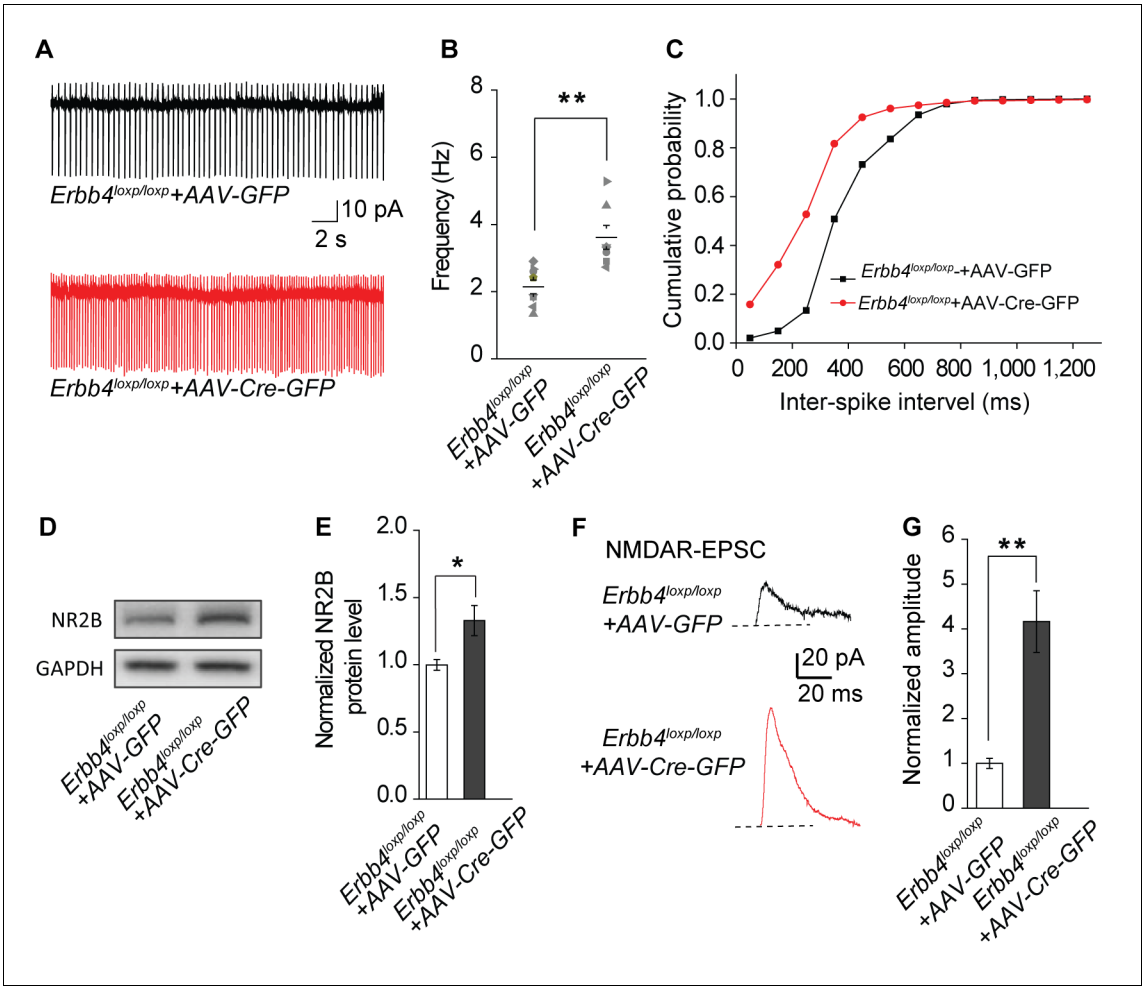

Figure 6. The spontaneous excitability, NR2B expression, and NMDAR current of LC-NE neurons are increased in *ErbB4*$^{loxp/loxp}$ mice bilaterally injected with AAV-Cre-GFP virus into the LC. (**A**) Representative spontaneous firing traces of LC-NE neurons in *ErbB4*$^{loxp/loxp}$ mice bilaterally injected with AAV-GFP or AAV-Cre-GFP virus. (**B**), (**C**) Quantification of firing frequency (**B**) and cumulative histogram of inter-spike interval (**C**) of spontaneous firing. n = 8 (*ErbB4*$^{loxp/loxp}$-AAV-GFP); n = 7 (*ErbB4*$^{loxp/loxp}$-AAV-Cre-GFP). (**D**), (**E**) Representative blot (**D**) and quantification (**E**) of NR2B protein level from LC protein lysates of *ErbB4*$^{loxp/loxp}$ mice received AAV-GFP or AAV-Cre-GFP injection. n = 3 (control); n = 3 (*Th-Cre; ErbB4*$^{loxp/loxp}$). (**F**), (**G**) NMDAR current is enhanced in *ErbB4*$^{loxp/loxp}$ mice bilaterally injected with AAV-Cre-GFP. n = 3 (*ErbB4*$^{loxp/loxp}$-AAV-GFP); n = 3 (*ErbB4*$^{loxp/loxp}$-AAV-Cre-GFP). Unpaired two-tailed Student's t-test and Two-sample Kolmogorov-Smirnov test. Data are expressed as means ± s.e.m. *p<0.05, **p<0.01.

DOI: https://doi.org/10.7554/eLife.39907.026

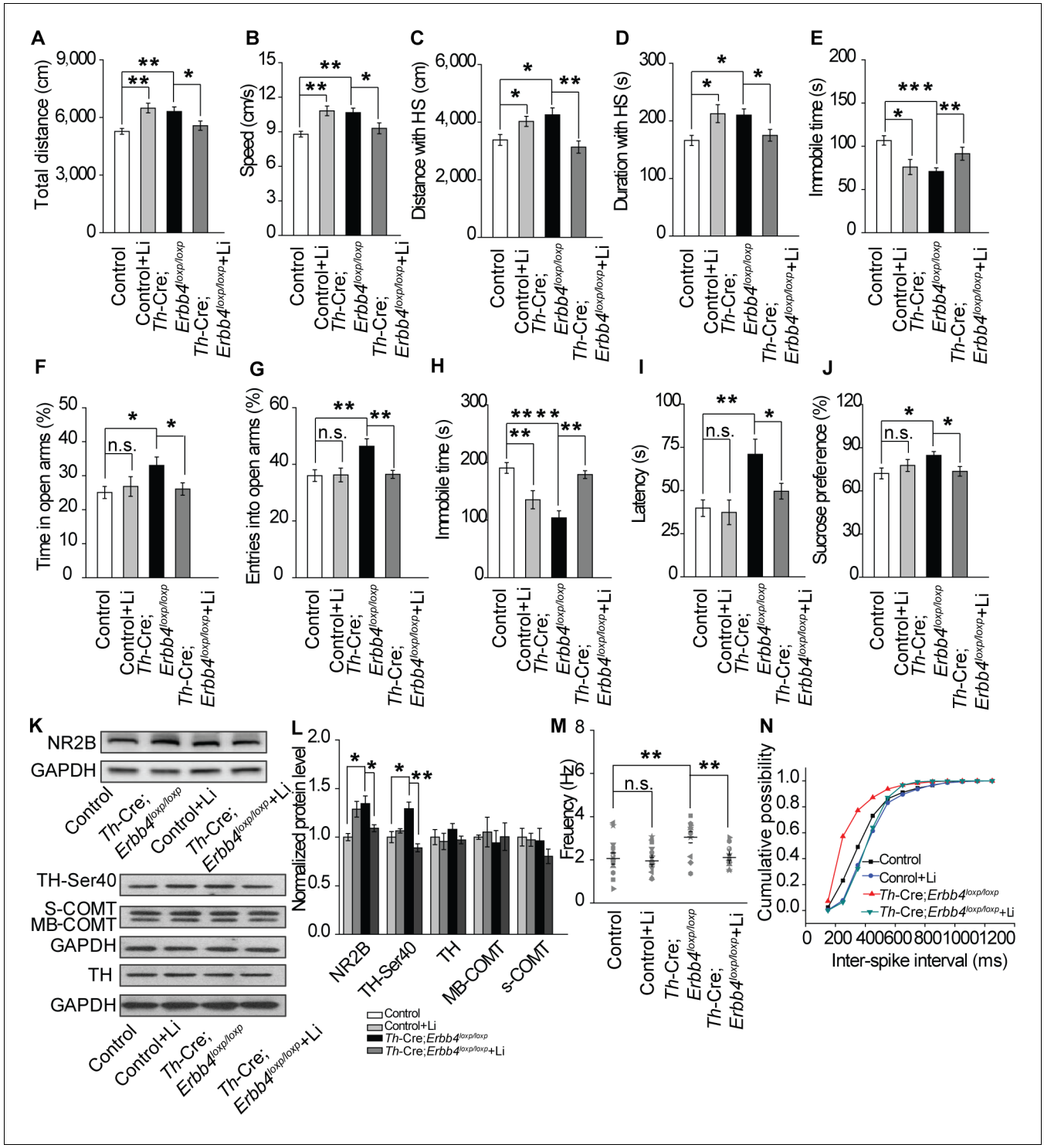

Figure 7. Lithium rescued the behavioral, molecular, and electrophysiological phenotypes of *Th-Cre;Erbb4*$^{loxp/loxp}$ mice. (**A**), (**B**) Locomotor activity (**A**) and speed (**B**) in the open field test. n = 24 (*Erbb4*$^{loxp/loxp}$), n = 10 (*Erbb4*$^{loxp/loxp}$ + lithium), n = 22 (*Th-Cre;Erbb4*$^{loxp/loxp}$), n = 13 (*Th-Cre;Erbb4*$^{loxp/loxp}$ + lithium). (**C–E**) Distance (**C**) and duration (**D**) traveled at HS and immobility time (**E**) after lithium treatment. (**F**), (**G**) Percentage of time (**F**) and entries (**G**) into open arms by *Th-Cre;Erbb4*$^{loxp/loxp}$ mice with and without lithium in the EPM test. n = 23 (*Erbb4*$^{loxp/loxp}$); n = 8 (*Erbb4*$^{loxp/loxp}$ + lithium); n = 24 (*Th-Cre;Erbb4*$^{loxp/loxp}$); n = 18 (*Th-Cre;Erbb4*$^{loxp/loxp}$ + lithium). (**H**), (**I**) Immobility time (**H**) and latency to first surrender (**I**) in forced swim test. n = 20 (*Erbb4*$^{loxp/loxp}$); n = 8 (*Erbb4*$^{loxp/loxp}$ + lithium); n = 16 (*Th-Cre;Erbb4*$^{loxp/loxp}$); n = 20 (*Th-Cre;Erbb4*$^{loxp/loxp}$ + lithium). (**J**) Sucrose preference of *Th-Cre;Erbb4*$^{loxp/loxp}$ mice treated with lithium. n = 19 (*Erbb4*$^{loxp/loxp}$); n = 12 (*Erbb4*$^{loxp/loxp}$ + lithium); n = 13 (*Th-Cre;Erbb4*$^{loxp/loxp}$); n = 16 (*Th-Cre;Erbb4*$^{loxp/loxp}$ + lithium). (**K**) Western blots of LC samples from *Th-Cre;Erbb4*$^{loxp/loxp}$ mice with and without lithium treatment. (**L**) Protein level of NR2B

Figure 7 continued on next page

Figure 7 continued

and TH-Ser40 in the LC after lithium treatment. Protein levels of TH, s-COMT, and MB-COMT were not significantly changed in the LC after lithium treatment. TH, tyrosine hydroxylase; S-COMT, soluble catechol-o-methyltransferase; MB-COMT, membrane-binding form of COMT. n = 4 (*Erbb4*$^{loxp/loxp}$); n = 4 (*Erbb4*$^{loxp/loxp}$ + lithium); n = 4 (*Th-Cre;Erbb4*$^{loxp/loxp}$); n = 4 (*Th-Cre;Erbb4*$^{loxp/loxp}$ + lithium). (**M**), Spontaneous firing of LC-NE neurons after lithium treatment. n = 13 from three mice (*Th-Cre;Erbb4*$^{loxp/loxp}$); n = 15 from three mice (*Th-Cre;Erbb4*$^{loxp/loxp}$ + lithium). (**N**) Interspike intervals after lithium treatment. n = 13 from three mice (*Th-Cre;Erbb4*$^{loxp/loxp}$); n = 15 from three (*Th-Cre;Erbb4*$^{loxp/loxp}$ + lithium). Two-way ANOVA. Data are expressed as means ± s.e.m. Two-sample Kolmogorov-Smirnov test and data in (**N**) are presented as a cumulative frequency plot. *p<0.05, **p<0.01, ****p<0.0001. n.s., not significant.

DOI: https://doi.org/10.7554/eLife.39907.028

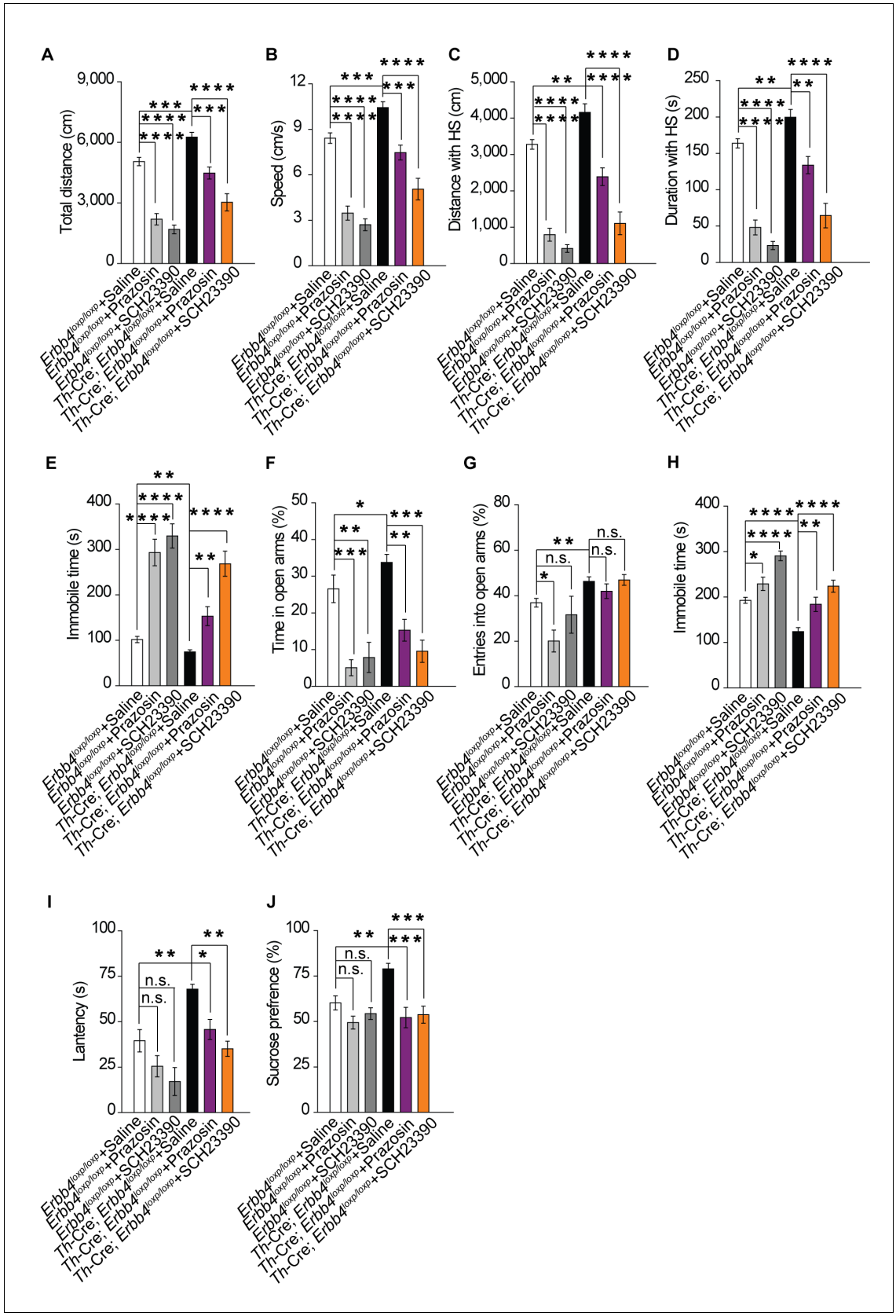

Figure 8. Increase in both norepinephrine and dopamine contribute to mania-like behaviors. (**A**), (**B**) Locomotor activity (**A**) and speed (**B**) of *Th-Cre; Erbb4*$^{loxp/loxp}$ mice treated with saline (sal), prazosin, or SCH23390 in open field test. n = 17 (*Erbb4*$^{loxp/loxp}$ + sal); n = 12 (*Erbb4*$^{loxp/loxp}$ + prazosin);

Figure 8 continued on next page

Figure 8 continued

n = 11 (*Erbb4*$^{loxp/loxp}$ + SCH23390); n = 11 (*Th-Cre;Erbb4*$^{loxp/loxp}$ + sal); n = 10 (*Th-Cre;Erbb4*$^{loxp/loxp}$ + prazosin); n = 9 (*Th-Cre;Erbb4*$^{loxp/loxp}$ + SCH23390). (**C**), (**D**) Distance (**C**) and duration (**D**) at HS in open field test. (**E**) Immobility time in open field test. (**F**), (**G**) Time (**F**) and entries (**G**) in open arms in EPM test. n = 11 (*Erbb4*$^{loxp/loxp}$ + sal); n = 12 (*Erbb4*$^{loxp/loxp}$ + prazosin); n = 11 (*Erbb4*$^{loxp/loxp}$ + SCH23390); n = 14 (*Th-Cre;Erbb4*$^{loxp/loxp}$ + sal); n = 11 (*Th-Cre;Erbb4*$^{loxp/loxp}$ + prazosin); n = 8 (*Th-Cre;Erbb4*$^{loxp/loxp}$ + SCH23390). (**H**), (**I**) Immobility time (**H**) and latency to first surrender (**I**) in forced swim tests. n = 12 (*Erbb4*$^{loxp/loxp}$ + sal); n = 10 (*Erbb4*$^{loxp/loxp}$ + prazosin); n = 10 (*Erbb4*$^{loxp/loxp}$ + SCH23390); n = 16 (*Th-Cre;Erbb4*$^{loxp/loxp}$ + sal); n = 12 (*Th-Cre;Erbb4*$^{loxp/loxp}$ + prazosin); n = 12 (*Th-Cre;Erbb4*$^{loxp/loxp}$ + SCH23390). (**J**) Sucrose preference of *Th-Cre;Erbb4*$^{loxp/loxp}$ mice after prazosin or SCH23390 treatment. n = 11 (*Erbb4*$^{loxp/loxp}$ + sal); n = 9 (*Erbb4*$^{loxp/loxp}$ + prazosin); n = 10 (*Erbb4*$^{loxp/loxp}$ + SCH23390); n = 11 (*Th-Cre;Erbb4*$^{loxp/loxp}$ + sal); n = 12 (*Th-Cre;Erbb4*$^{loxp/loxp}$ + prazosin); n = 12 (*Th-Cre;Erbb4*$^{loxp/loxp}$ + SCH23390). One-way ANOVA and Tukey's multiple comparison test. Data are expressed as means ± s.e.m. *p<0.05, **p<0.01, ***p<0.001, ****p<0.0001. n.s., not significant.

DOI: https://doi.org/10.7554/eLife.39907.030